Study of solid phase sintering of chromite ore pellets via the methods of non-isothermal kinetics

A. K. Zhunusov, *Cand. Eng., Associate Prof., Head of the Dept. "Metallurgy"* [1], *e-mail: zhunusov_ab@mail.ru;*
E. E. Abdulabekov, *Cand. Eng., Plant Director* [2];
P. O. Bykov, *Cand. Eng., Associate Prof., Dept. "Metallurgy"* [1], *e-mail: bykov_petr@mail.ru;*
A. E. Kenzhebekova, *Senior Lecturer, Dept. "Metallurgy"* [1], *e-mail: kenzhebekova_psu@mail.ru;*
A. K. Zhunusova, *Doctoral Candidate, Dept. "Metallurgy"* [1, 3], *e-mail: zhunusova.aig@mail.ru*

[1] *Toraigyrov University (Pavlodar, Kazakhstan)*
[2] *Aktyubinsk Ferroalloy Plant (Aktobe, Kazakhstan)*
[3] *Pavlodar Machine-Building College (Pavlodar, Kazakhstan)*

The method of thermal effect of reactions for E_{act} calculation for the processes of chromite ore and clay interaction in solid phase was used in this research for obtaining kinetic data. These processes take place during hardening roasting of chromite ore pellets in derivatograph Q-1500. The samples of chromite ore, clay from Sazdinskoe deposit (Aktyubinsk region, Kazakhstan) and pellets were taken for examination of phase transformations during hardening roasting. In the area of high temperatures, exothermic peaks with temperature maximum values 1340 and 1430 °C are clearly observed on the differential and thermal curve of chromite ore; these maximal values are caused by recrystallization of chromium spinellid grains. Introduction of clay changes the features of diffusion processes in chromite ore. Observed lowering of apparent activation energy for each peak is separately connected with decrease of diffusion retarding processes. When conducting an experiment in argon neutral atmosphere, distinct peaks characterizing diffusion processes and reconstruction of chromium spinellid lattice are not observed. In this case, the value of apparent activation energy decreases seriously in comparison with activation energy of diffusion processes for the mix of chromite ore and clay in oxidizing atmosphere. Respectively, hardening processes during heat treatment of pellets, which are accompanied by diffusion of clay oxides in chromium spinellid lattice, will pass with rather high speed and will reach high degree of completeness at the roasting temperature of pellets (1200–1300 °C).
Key words: chromite ore, pellets, diffusion, non-isothermal kinetics, oxidizing atmosphere, chromium spinellids, activation energy.
DOI: 10.17580/cisisr.2025.01.02

Introduction

About 70–80 % of total mining volume of chromite ore at Donskoy mining and concentrating plant (Khromtau, Kazakhstan) is estimated for fine chromite ore (less than 20 mm). This plant is the main raw material base of ferroalloy plants in Kazakhstan. Use of fine ores in metallurgical production makes melting processes more difficult and rises energy expenses. Fine-dispersed materials are carrying away from technological equipment via blowing and make complications in operation of gas cleaning systems. Thereby large amount of initial ores at Kempirsaiskoe deposit in Kazakhstan, as well as part of enriched concentrates become practically inapplicably for direct use in technological processes and require special preparing processing – agglomeration.

Analysis of global experience of preparation of chromite ores to metallurgical processing displayed that pelletizing and briquetting are the most widely distributed and successfully used agglomeration methods abroad. It should be noted that roasting of pellets is more preferable method at present time in comparison with briquetting, which was widely used in 1970-ies. Despite successful use and distribution of pelletizing of chromite ores abroad, it should be mentioned that ores from domestic and foreign deposits differ substantially [1–5].

Taking into account the above-mentioned parameters, the experiments for pelletizing of fine fractions of chromite ore (0–1 mm) from Kempirsaiskoe deposit, using keramzite clay, were carried out. To understand the complete nature of this process, it is necessary to conduct investigations for revealing the temperature maximum values and the value activation energy for chromite ore and composition of chromite ore with clay. Determination of these values will allow to testify that diffusion processes, occurring during heat treatment and responsible for hardening of sintered materials with clay participation, will pass at favourable conditions. However, information about kinetic parameters of interaction process between chromite ore and clay during hardening roasting (in particular, activation energy) is required for studying and optimizing the temperature and temporal procedure of hardening roasting of chromite ore pellets.

At present time, the new methods for examination of solid phase reactions, including those for determination of

apparent activation energy in the conditions of heating of reactants with permanent speed, were developed. The following methods can be mentioned here: differential and thermal analysis (DTA), thermal gravimetric analysis (TGA) and differential thermal gravimetric analysis (DTGA). TGA and DTGA methods are widely used for examination of phase transitions, dissociation reactions, reduction, oxidation, dehydration and other processes connected with varying of enthalpy and mass of a substance. Possibility of determination of all kinetic constants (E_{act}, A and n) during one experiment is a real advantage of the method of non-isothermal kinetics.

Solving the system of two equations, connecting the constant of reaction speed k and the temperature T and the reaction speed V with transformation degree α is a general approach for the task of determination of kinetic parameters:

$$k = A \cdot \exp(-E_{act} RT) \quad (1)$$

$$V = kf(\alpha) \quad (2)$$

where E_{act} – activation energy of the process;

A – pre-exponential multiplier, which does not depend on the temperature within a small temperature range;

R – a gas constant; it is expresses by the equation $V = k(1-\alpha)^n$, where n – is reaction order, for the case with decomposition of solid substances.

Activation energy E_{act} is determined via the tangent of inclination angle for the relationship $\lg k = f(1/T)$, which was obtained via taking the logarithm of the Arrenius equation (*1*) [6]. To determine the constant of reaction speed k, it is necessary to carry out the series of experiments at different temperatures for isothermal conditions, with continuous registration of mass loss.

Technical literature [7–10] describes the techniques, which allow to determine activation energy of the processes after data processing for the curves via TGA or DTA methods. The most of above-listed methods are connected with selection of n values and requires labour-intensive calculations. More simple calculation method was suggested by H. E. Kisinger [11], which is based on determination of the maximal temperature (T_{max}) and the DTA curve form index. However, it is not always possible to determine this index due to its deviation from the zero line. H. E. Kisinger also suggested the method for E_{act} determination, when thermograms of the same substance are recorded for different heating temperatures and the corresponding graph with coordinates $\ln b/T_m^2 - 1/T$, where T_m – peak temperature in K, is built based on these thermograms.

The work [12] proposes to make easier solving the task of assessing E_{act} values using the DTGA curves obtained via derivatograph. DTGA curve reflects the relationship between speed of mass varying and temperature rise. In this connection, technological speed can be determined for each temperature, and this speed is calculated as follows:

$$V = \frac{h \cdot l \cdot p_0}{\tau_0 \cdot S_0} \quad (3)$$

where V – speed of mass loss for concrete time, g/s;

h – deviation of DTGA curve from the zero horizontal line, mm;

l – length of zero line, mm;

p_0 – sample mass, mg;

τ – experiment duration, s;

S_0 – square restricted by DTGA curve and zero line, mm.

Thus, the graph with coordinates $\lg V - 1/T$ was built after determination of the values of technological speed and temperature with definite time interval using a thermogram. The straight section of this relationship is characterized by the following equation: $V = B_{exp}(-E_{act}/RT)$. Activation energy E_{act} is determined via the tangent of inclination angle of the straight section, while the section, which is cut by continuation of the straight line on the ordinate axis, is proportional to the B value.

The research [13] suggested to conduct processing of thermograms via determination of transformation degree by mass loss and varying of enthalpy by thermal effect peak square in order to examine metallurgical processes characterizing by mass loss (decomposition of carbonates, carbothermic reduction of metals etc.) via the methods of isothermal kinetics. However, use of this method is restricted by the processes accompanying by mass loss, they don't relate to solid phase reactions without mass loss.

Other researches [14, 15] are devoted to kinetic regularities of the processes by reaction thermal effect, which is evaluated by square of the corresponding DTA peak. Exact square measuring is complicated, because downward branch of DTA curve not always correspond to the zero line, so special restriction techniques should be used [16]. Different methods of square restriction lead to deviation in the results up to 20 % and, respectively, to decrease of precision in determination of activation apparent energy.

This method is based on the idea that the value of heat absorption by the system in the area from fixed beginning with maximal process development, in the conditions of heating with permanent speed, is proportional to the constant of transformation speed for each temperature value in isothermal conditions. Indeed, the authors of [17] underlined that analysis of thermal effects in exothermic reactions should take into account that the maximum point of DTA curve coincides with the moment of reaction finishing; thereby, we should use not more than 50 % of the peak in practical calculations.

These arguments were the cause of searching a method for determination of activation apparent energy by one thermogram; this method does not include DTA peak square, curve form index, reaction order in calculation. The main equation of non-isothermal kinetics for solid phase reactions is expressed as follows:

$$d\alpha / dT = (A/b)\left[f'(\alpha)\right]e^{-E/RT}; f'(\alpha) = (1-\alpha)^n \quad (4)$$

The equation (4) is obtained from the formal kinetic equation of solid phase reaction

$$d\alpha / d\tau = k(1-\alpha)^n \quad (5)$$

of temperature relationship of a speed constant, so called Arrenius equation

$$k = A \cdot e^{-E/RT} \quad (6)$$

and the equation of temperature varying for constant heating speed

$$T = T_0 + b\tau, \mathrm{d}T / d\tau = b \quad (7)$$

where α – transformation degree;
n – reaction order;
E – activation energy;
A – pre-exponential multiplier;
b – heating speed.

It is known that the thermal curve more and more deviates from the preset state AC as soon as reaction in a sample is developing (**Fig. 1**). The value of this deviation Δt (*ab*, *cd* etc.) is described by the following formula in first approximation:

$$\Delta t \approx \Delta S \frac{d\alpha}{d\tau} \quad (8),$$

where ΔS – square under DTA curve during its deviation from the basic line and consequent return to it (square *ABC* on the Fig. 1).

Indeed, deviation of DTA curve from the preset direction Δt (when $\mathrm{d}T / d\tau = b$) in the initial section of substance transformation is determined only by reaction speed.

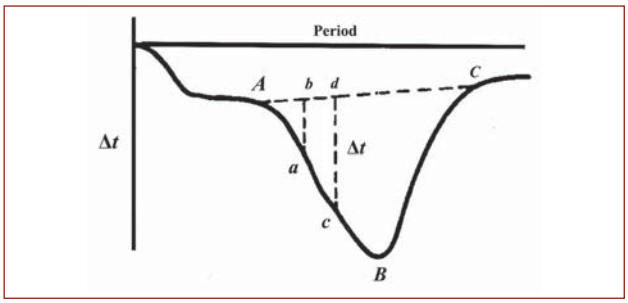

Fig. 1. Thermal effect and its parameters

If we take a logarithm by the expression (8), taking into account the equation (4), we shall obtain the following expression:

$$\ln\Delta t = C + n\ln(1-\alpha) - \frac{E_{act}}{RT} \quad (9)$$

where $C = \Delta S \cdot A / b$ – coefficient uniting all permanent components of the equations (4) and (8). For small α values, we can neglect the value $n\ln(1-\alpha)$ and the equation (9) will be as follows:

$$\ln\Delta t = C - E_{act} / RT \quad (10)$$

Using the equation (10), which provide connection between deviation of differential record from zero state and apparent activation energy, we can calculate E_{act} value via tangent of inclination angle of direct relationship of deviation from basic DTA curve in the coordinates $\lg\Delta t - 1 / T$.

The aim of this research is use of the methods of non-isothermal kinetics for experimental determination of the values of energy activation during hardening roasting processes of chromite ores and pellets. This work proposes to use the method of thermal effect in the reaction for Eact calculation for interaction processes of chromite ore and clay in solid phase, occurring during hardening roasting of chromite ore pellets.

Materials and methods

To obtain DTA curves, a derivatograph Q-1500 was used. The samples of chromite ore and clay from Sazdinskoe deposit (Aktyubinsk region, Kazakhstan), as well as pellets obtained in laboratorial conditions were taken as initial materials for examination of phase transformations taking place during hardening roasting.

When manufacturing pellets, choosing the most suitable and cheap binding material is one of the main tasks. This material should not lead to cost rise of pellets in production conditions. Keramzite clay from Sazdinskoe deposit was selected as such cheap binding material.

Based on the data of X-ray structural analysis [18], kaolinite ($Al_2O_3 \cdot 2SiO_2 \cdot 2H_2O$), quartzite ($SiO_2$) and feldspar are presented in keramzite clay. Respectively, keramzite clay from Sazdinskoe deposit can be classified to the kaolinite group, which is characterized by low bloating and relatively high softening temperature.

Chemical composition of keramzite clay from Sazdinskoe deposit, chromite clay and pellets is presented in the **Table 1** and **Table 2**.

Laboratorial experiments for pelletizing of chromite ore using keramzite clay were carried out in a disk granulator with 1,000 mm diameter. The part of binding additive (clay) was varied within the range from 1 to 10 %. Fractional composition of materials is presented in the **Table 3**.

The results of experiments for examination of influence of keramzite clay additives and roasting temperature on strength of pellets are presented in the **Fig. 2**.

Fig. 2 displays that strength of chromite ore pellets remains low at the roasting temperatures 1000 °C and 1100 °C. Varying of strength of pellets starts from the temperature 1200 °C and higher, and then maximal strength value is achieved. Thereby it can be concluded that introduction of 8 % of keramzite clay in composition of pellets is rather optimal.

The conducted laboratorial experiments for manufacture of green and roasted pellets of chromite ore display principal possibility to obtain chromite pellets with keramzite clay additive.

It is known [18], that chromite ore consists of chromium spinellid and rock-forming cementing mineral – serpentine ($3MgO \cdot 2SiO_2 \cdot 2H_2O$). X-tay phase analysis, which was carried out by the authors, did not reveal serpentine (previously presented in chromite ore) in roasted pellets. Composition of

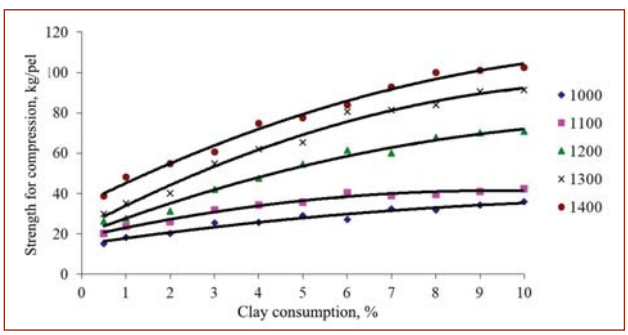

Fig. 2. Influence of hardening roasting temperature and clay consumption on strength of chromium ore pellets

Table 1. Chemical composition of chromite ore and clay

Material	Chemical composition, %								
	Cr_2O_3	SiO_2	CaO	MgO	Al_2O_3	FeO	P	S	other
Chromite ore	47.76	8.65	0.24	19.87	6.99	12.11	0.0023	0.026	2.93
Clay	1.07	51.53	2.36	5.41	18.14	7.83	0.16	0.29	7.14

Table 2. Chemical composition of pellets

Material	Chemical composition, %								
	Cr_2O_3	SiO_2	CaO	MgO	Al_2O_3	FeO	P	S	other
Pellets	43.27	12.79	0.29	21.88	7.08	11.30	0.0036	0.034	2.03

Table 3. Fractional composition of chromite ore and keramzite clay

Material	Size of sieves, mm											
	+2.5	+1.6	+1.0	+0.63	+0.4	+0.31	+0.2	+0.16	+0.1	+0.063	+0.05	-0.05
Ore	11.38	8.32	6.28	6.95	10.51	5.85	14.53	8.68	16.47	7.52	2.47	1.03
Clay	0	0	0	0	0	15.14	63.82	10.63	7.26	1.26	1.89	0

pellets also includes quartzite (brought in by clay and formed as a result of serpentine decomposition).

Researches and their results

To examine the processes taking place during hardening roasting of pellets, derivatographic investigations of materials were conducted (see **Table 4**).

Endothermic effect within the temperature range 70–140 °C, which is observed during heating of a clay sample, characterizes deletion of natural moisture (**Fig. 3**). Hydrate moisture of a clay mineral (kaolin) is deleted at 523 °C and organic clay impurities are oxidized and burnt at the temperatures 455–540 °C.

Analysis of thermograms of other materials (**Table 4, Fig. 4**) allowed to obtain thermal effects presented in the **Table 5**. It shows that five typical peaks are observed in thermograms of chromite ore and clay. At the same time, thermal effects No. 2–5 are not seen in the thermogram of pellets. Respectively, this circumstance allows to testify that all processes during hardening roasting of pellets pass rather completely.

The first endothermic effect at the temperatures 90–150 °C corresponds to loss of adsorbed water (see Fig. 4, *a-c*).

The second endothermic effect at the temperatures 640–695 °C corresponds to extraction of "structural" water from serpentines (antigorite and chrysotile), during its decomposition with forming of forsterite, quartzite and water (see Fig. 4, *a-c*) according to the following reaction:

$$2Mg_3Si_2O_5(OH) = 3Mg_2SiO_4 + SiO_2 + 4H_2O$$

where SiO_2 is presented as amorphous silica in the product of serpentine decomposition [19].

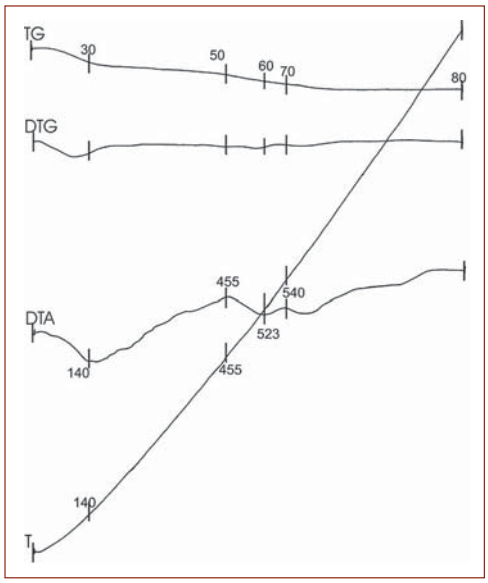

Fig. 3. Thermogram of clay, captured within the temperature range 20–1000 °C in the air atmosphere

The following exothermic effect within the temperature range 770–820 °C is stipulated in thermograms by forming of enstatite $MgSiO_3$ from serpentine decomposition products [20–23].

This exothermic peak is rather different in its value. Perhaps, dehydration process is replaced by enstatite forming so quickly, that exothermic pear is overlapped by endothermic one and decreased due to endothermic effect.

As for the high-temperature area, two exothermic peaks with the temperature maximums 1340 and 1430 °C, which are caused by recrystallization of chromium spinellid grains,

Table 4. Capturing procedure with derivatograph

No.	Material	Heating speed, grad/min	Maximal temperature, °C	Atmosphere
1	Clay	10	1000	Air
2	Chromite ore	15	1500	Air
3	Chromite ore + 8% clay	15	1500	Air
4	Chromite ore + 8% clay	15	1500	Argon
5	Pellets	15	1500	Argon

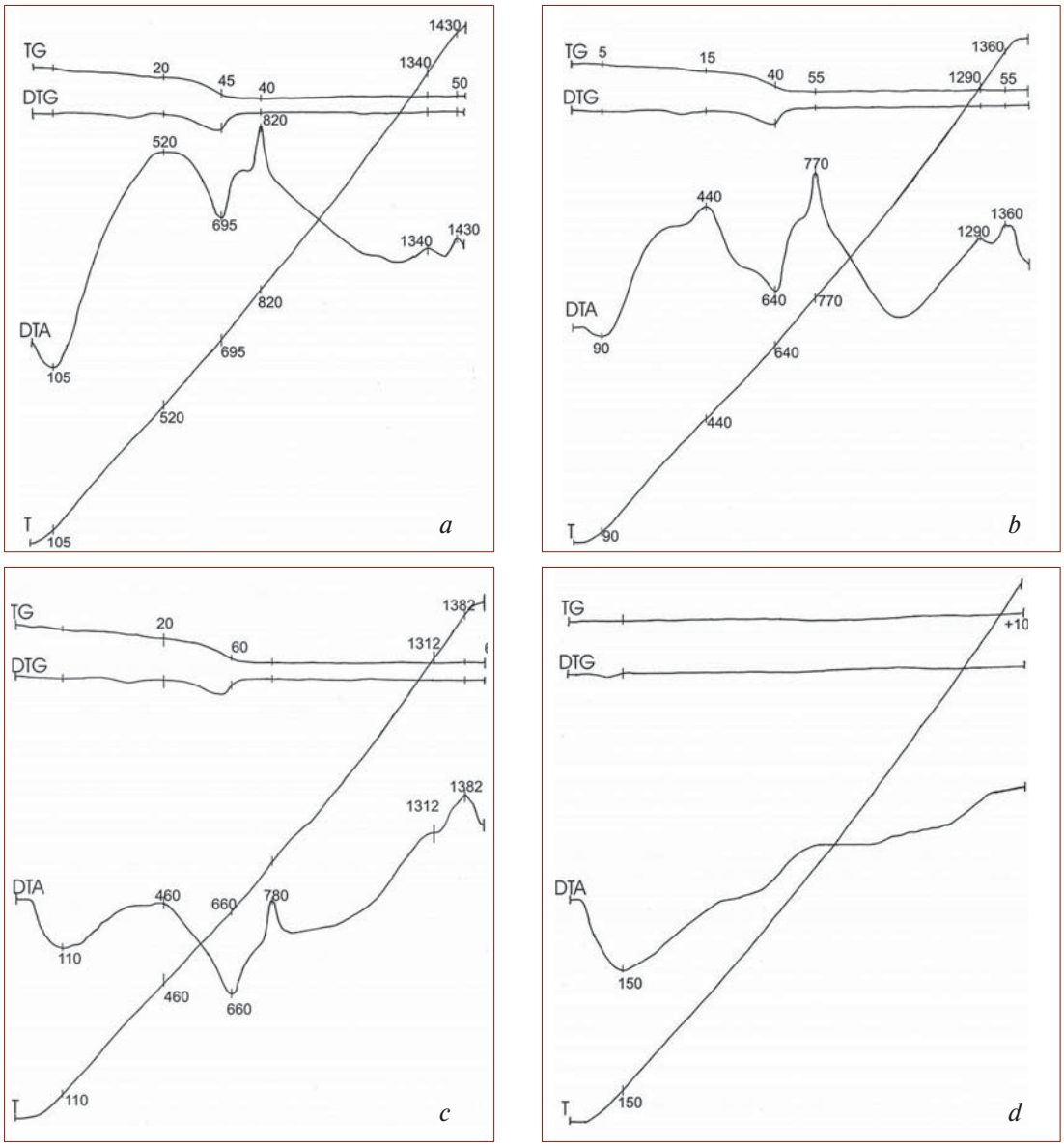

Fig. 4. Thermograms of examined materials: *a* – chromite ore; *b* – chromite ore + clay; *c* – chromite ore + clay in argon atmosphere; *d* – pellets

Table 5. Thermal effects, °C

No.	Materials from the Table 4				Comment
	2	3	4	5	
1	105	90	110	150	Deletion of natural moisture
2	695	640	660	–	Decomposition of serpentine
3	820	770	780	–	Forming of olivine
4	1340	1290	1312	–	Rebuilding of chromium spinellid lattice
5	1430	1340	1382	–	

are seen clearly on the differential and thermal curve of chromium ore (see Fig. 4, *a*). Separation of peaks testifies on conducting of consequent reactions.

Introduction of clay changes the features of diffusion processes in chromite ore. The exothermic peak in thermograms of chromite ore and clay both in air and argon atmospheres starts from more low temperatures (1036 °C in the air and 969 °C in argon atmosphere) and passes within more wide temperature range 200–300 °C. This pear is caused by occurring solid phase exothermic reactions (1) – (7) with forming of cordierite and enstatite. They are overlapped mutually in the thermogram captured in argon atmosphere for chromite ore and clay (see Fig. 4, *c*). Calculation results are displayed in the **Table 6**.

Thus, the conducted derivatographic investigations of interaction between chromite ore and keramzite clay provided experimental confirmation of conclusions in the form of thermodynamic and diagram analysis on possibility of

Table 6. Values of apparent activation energy, which was determined by the tangent of inclination angle of $\lg\Delta t - 1/T$ direct relationship

No.	Material	Atmosphere	Equation	R	E_{act}, kJ/mol	Temperature range, °C
1	Chromite ore	Air	$\ln\Delta t = -748.54/T + 9.8956$	0.988	14.33	547–695
			$\ln\Delta t = -4840.6/T + 52.8069$	0.979	92.68	782–820
			$\ln\Delta t = -3487.7/T + 22.3061$	0.986	66.78	1259–1340
			$\ln\Delta t = -9389.9/T + 56.9126$	0.954	179.79	1396–1430
2	Chromite ore + clay	Air	$\ln\Delta t = -1131.7/T + 13.7334$	0.985	21.67	580–640
			$\ln\Delta t = -3684.4/T + 37.1595$	0.964	70.54	735–770
			$\ln\Delta t = -1217.9/T + 9.9932$	0.940	23.32	1036–1290
			$\ln\Delta t = -7704.1/T + 48.7950$	0.955	147.51	1294–1340
3	Chromite ore + clay	Argon	$\ln\Delta t = -874.6/T + 10.3110$	0.962	16.75	574–660
			$\ln\Delta t = -2932.3/T + 29.0930$	0.994	56.15	716–780
			$\ln\Delta t = -986.2/T + 7.3839$	0.967	18.88	969–1312
			$\ln\Delta t = -5049.2/T + 31.5156$	0.919	96.68	1325–1382

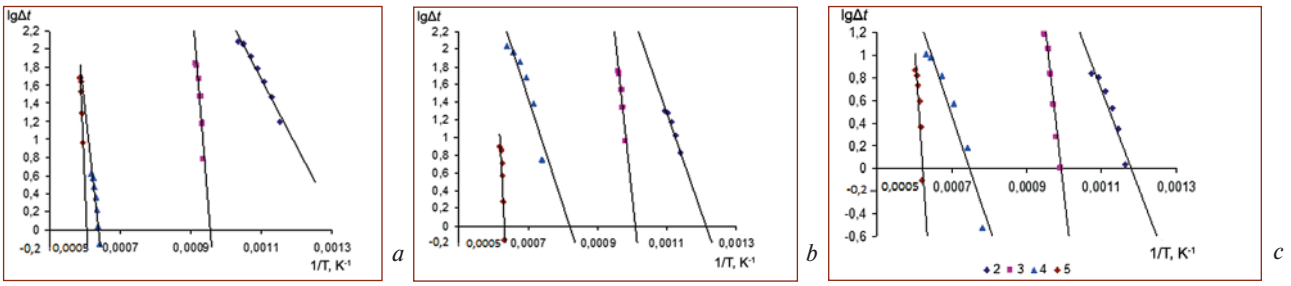

Fig. 5. Relationship of DTA peak height in semi-logarithmic coordinates from reverse temperature: *a* – chromite ore; *b* – chromite ore + clay; *c* – chromite ore + clay in argon atmosphere; numbers of peaks under the figures see in the Table 5

solid phase reactions on composition of pellets, which will promote hardening of pellets due to cordierite forming. These reactions start at 1036 °C and finish at 1360 °C.

Based on the determination of the temperature values and DTA curve deviation value from preset direction, relationships in the coordinates $\lg\Delta t - 1/T$ for each thermal effect were built according to the data from the Table 4, and E_{act} values of the processes corresponding to peaks in thermograms were calculated by the tangent of inclination angle $\lg\Delta t - 1/T$ of direct relationship. The results of linearization of the upward branch of DTA peak in the coordinates $\lg\Delta t - 1/T$ are presented in the **Fig. 5**.

Analysis of the temperature maximums and activation energy level for technological processes are accompanied by peaks for DTA curves of chromite ore and composition of chromite ore with clay (Table 6). It allows to testify that reactions occurring during heat treatment and responsible for hardening of sintered materials with clay participation take place in favourable conditions.

Thus, the observed lowering of apparent activation energy for each peak separately is connected with decrease of diffusion retarding processes. When conducting an experiment in argon neutral atmosphere, distinct peaks characterizing diffusion processes and reconstruction of chromium spinellid lattice are not observed (see Fig. 2, *c*). In this case, the value of apparent activation energy decreases seriously in comparison with activation energy of diffusion processes for the mix of chromite ore and clay in oxidizing atmosphere. Respectively, hardening processes during heat treatment of pellets, which are accompanied by diffusion of clay oxides in chromium spinellid lattice, will pass with rather high speed and will reach high degree of completeness at the roasting temperature of pellets (1200–1300 °C).

Conclusions

1. Activation energy of the processes occurring during hardening roasting of chromite ore and pellets (on the example of the mixture of chromite ore and clay) in oxidizing and neutral atmosphere was determined on the base of conducted researches via the method of non-isothermal kinetics.

2. Analysis of the temperature maximums and activation energy level for technological processes are accompanied by peaks for DTA curves of chromite ore and composition of chromite ore with clay. It allows to testify that reactions occurring during heat treatment and responsible for hardening of sintered materials with clay participation take place in favourable conditions. Respectively, it can be concluded that hardening processes during heat treatment of pellets, which are accompanied by diffusion of clay oxides in chromium spinellid lattice, will pass with rather high speed and will reach high degree of completeness at the roasting temperature of pellets (1200–1300 °C).

REFERENCES

1. Xianfeng Hu, Sundqvist Ökvist L., Eriksson J., Qixing Yang, Björkman B. Direct Alloying Steel with Chromium by Briquettes Made from Chromite Ore, Mill Scale, and Petroleum Coke. *Steel research international*. 2017. Vol. 88. No. 5. pp. 1–10. DOI: 10.1002/srin.201600247.
2. Kleynhans E. L. J., Beukes J. P., Van Zyl P. G., Fick J. I. J. Techno-economic feasibility of a pre-oxidation process to enhance prereduction of chromite. *Journal of the Southern African Institute of Mining and Metallurgy*. 2017. Vol. 117. No. 5. pp. 457–468. DOI: 10.17159/2411-9717/2017/v117n5a8.
3. Beukes J. P., Du Preez S. P., Van Zyl P. G., Paktunc D., Fabritius T., Päätalo M., Cramer M. Review of Cr (VI) environmental practices in the chromite mining and smelting industry-relevance to development of the Ring of Fire, Canada. *Journal of Cleaner Production*. 2017. Vol. 165. pp. 874–889. DOI: 10.1016/j.jclepro.2017.07.176.
4. Du Preez S. P., Beukes J. P., Paktunc D., Van Zyl P. G., Jordaan A. Recycling pre-oxidized chromite fines in the oxidative sintered pellet production process. *Journal of the Southern African Institute of Mining and Metallurgy*. 2019. Vol. 119 (2). pp. 207–215. DOI: 10.17159/2411-9717/2019/v119n2a13.
5. Du Preez S. P., Beukes J. P., Van Zyl P. G., Tangstad M., Tiedt L. R. Silicon carbide formation enhanced by in-situ-formed silicon nitride: an approach to capture thermal energy of co-rich offgas combustion. *Metall Mater Trans, B*. 2018. Vol. 49 (6). pp. 51–63. DOI: 10.1007/s11663-018-1413-6.
6. Zhunusov A. K., Bykov P. O., Kenzhebekova A. E., Zhunussova A. K., Nabawi R. A. Study of the isothermal kinetics of reduction of sinter from mill scale. *Kompleksnoe ispolzovanie mineralnogo syrya*. 2024. Vol. 328 (1). pp. 59–67.
7. Serikbayeva A. K., Zhumashev K., Janaliyeva N. Sh., Rakhimberdina M. Definition of apparent activation energy on DTG curves. *Metalurgija*. 2016. Vol. 55 (3). pp. 417–419.
8. Ferapontov Yu. A., Putin S. B., Ferapontov L. L., Putin P. Yu. Study of kinetics of topochemical processes in non-isothermal procedure via derivatographic method. *Vestnik TGTU*. 2009. Vol. 15 (4). pp. 207–212.
9. Kelamanov B., Sariev O., Akuov A., Sultamuratova Z., Orynbassar R. Study of nickel briquettes by thermographic method. *Metalurgija*. 2022. Vol. 61 (1). pp. 217–220.
10. Vorobkalo N. R., Makhambetov Y. N., Baisanov A. S., Zayakin O. V. Study of possibility of manufacture of the complex titanium-containing ferroalloy via single-stage carbothermal method. *CIS Iron and Steel Review*. 2022. Vol. 24. pp. 17–23.
11. Towards improved thermal stability of negative electrode materials: differential scanning calorimetry and high-temperature X-ray diffraction/X-ray absorption spectroscopy in situ studies of $Li_2ZnTi_3O_8$ and related compounds. *ACS Applied Materials & Interfaces*. 2023. Vol. 15 (12). pp. 15605–15615. DOI: 10.1021/acsami.3c01123.
12. Sivasankara Rao Ede, Ananthakumar Ramadoss, Anantharaj S., Nithiyananthama U., Subrata Kundu. Influence of heat sintering on the physical properties of bulk $La_{0.67}Ca_{0.33}MnO_3$ perovskite manganite: role of oxygen in tuning the magnetocaloric response. *Physical Chemistry Chemical Physics*. 2014. Vol. 16. pp. 21846–21859.
13. Piecha J., Dabioch M., Breuer U., Leonarska A. Structural and electrical features induced by the leaching procedures on the $LiNbO_3$ crystalline powder samples. *Phase Transitions*. 2017. Vol. 90. No 1. pp. 34–43. DOI: 10.1080/01411594.2016.1206541.
14. Nadeem S., Hussain S. T., Changhoon Lee. Flow of a Williamson fluid over a stretching sheet. *Brazilian Journal of Chemical Engineering*. 2013. Vol. 30. No. 03. pp. 619–625. DOI: 10.1590/S0104-66322013000300019.
15. Ashraf M., Ahmad U., Chamkha A. J. Computational analysis of natural convection flow driven along curved surface in the presence of exothermic catalytic chemical reaction. *Comput. Therm. Sci*. 2019. No. 11. pp. 339–351.
16. Maleque Kh. A. Effects of Exothermic/Endothermic Chemical Reactions with Arrhenius Activation Energy on MHD Free Convection and Mass Transfer Flow in Presence of Thermal Radiation. *Journal of Thermodynamics*. 2013. Article ID 692516, 11 pages. DOI: 10.1155/2013/692516.
17. Tolymbekova L. B., Kim A. S., Zhunusov A. K., Babenko A. A. Thermal Transformations in Manganese Ores in the Zapadnyi Kamys Deposit and Chare Materials Used to Produse in an Air Flow under Nonisotherval Conditions. *Metallurgist*. 2013. Vol. 56. pp. 919–924.
18. Akuov A., Samuratov Y., Kelamanov B., Zhumagaliyev Y., Taizhigitova M. Development of an alternative technology for the production of refined ferrochrome. *Metalurgija*. 2020. Vol. 59 (4). pp. 529–532.
19. Abdulabekov E. E., Grinenko V. I., Izbembetov D. D. Manufacture of chromite pellets for melting of high-carbon ferrochromium. *Stal*. 2023. Vol. 5. pp. 39–41.
20. Saveliev D. E., Makatov D. K., Portnov V. S., Gataullin R. A. Morphology and textural-structural features of chromite deposits in the main ore field of Kempirsaisky massif (South Ural, Kazakhstan). *Georesursy*. 2022. Vol. 24. No. 1. pp. 62–73. DOI: 10.18599/grs.2022.1.6.
21. Saveliev D. E. Chromites of the Kraka ophiolite (South Urals, Russia): geological, mineralogical and structural features. *Mineralium Deposita*. 2021. vol. 56. pp. 1111–1132. DOI: 10.1007/s00126-021-01044-5.
22. Grishin I. A., Knyazbaev Zh. A. Analysis of modern state of theory and practice of chromite ores beneficiation. A review. *Kompleksnoe ispolzovanie mineralnogo syrya*. 2017. No. 1. pp. 10–15.
23. Orlov A. S., Isagulov A. Z., Sariev O. R., Tolymbekov M. Zh. Production of Aluminum-Chromium-Silicon Alloy from Unconditioned Materials. *Steel inTranslation*. 2018. Vol. 48 (9). pp. 558–563.